

1
2
3
4
5
6
7
8
9
10
11
12
13
14
15
16
17

Supplementary Information

UiO-66 metal-organic frameworks-derived ZrO₂/ZnO mesoporous material for high-efficiency detection towards NO₂ at room temperature

Jinhong Yang^a, Haoran Peng^a, Chong Lin^a, Qingjiang Pan^a, Lixue Qi^a, Li Li^{*ab}, and Keying Shi^{*a}

^a Key Laboratory of Functional Inorganic Material Chemistry, Ministry of Education, School of Chemistry and Material Science, Heilongjiang University, Harbin 150080, P.R. China

^b College of Modern Agriculture and Ecological Environment, Heilongjiang University, Harbin 150080, P. R. China

***Corresponding author**

Tel.: +86 451 86604920; +86 451 86609141

Email: lili1993036@hlju.edu.cn, shikeying2008@163.com

18 **Table S1** Comparison of gas-sensing performance of ZrO₂, ZnO and other hybrid
 19 materials to NO₂ gas with previous reports.

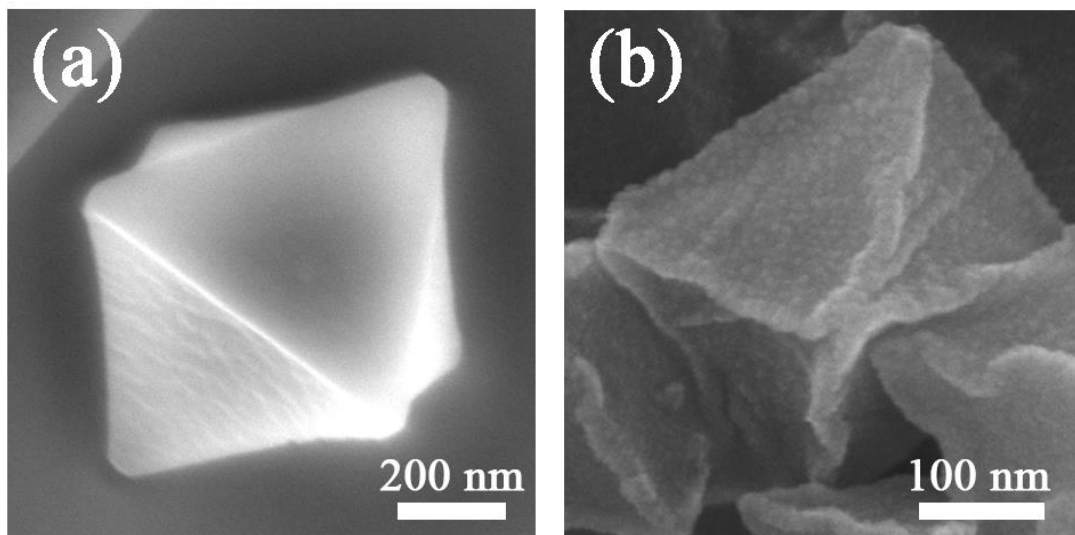
Sensor material	Gas	Operating temperature	Gas concentration	Response (s)	Response time	Recovery time	Detection limit	Ref.
SnO ₂ -ZrO ₂	NO ₂	150°C	10 ppm	24.7 ^①	-	-	-	1
ZrO ₂ -Y ₂ O ₃ (8%)	H ₂	150°C	1000 ppm	7.3 ^①	5 s	7 s	-	2
In ₂ O ₃ /ZrO ₂	C ₃ H ₆ O	260°C	100 ppm	60.38 ^①	1 s	38 s	10 ppm	3
SnO ₂ /ZrO ₂	TEA	190°C	20 ppm	4 ^①	1 s	1 s	-	4
NiO/ZnO	ethanol	260°C	100 ppm	61 ^①	-	-	-	5
Ag/ZnO	NH ₃	150°C	10 ppm	29.5 ^①	13 s	20 s	10 ppm	6
MXene/GO/CuO /ZnO	NH ₃	RT	200 ppm	96% ^②	-	-	4.1 ppm	7
ZnO/TiO ₂	NO ₂	500°C	50 ppm	7.5 ^①	-	-	-	8
Al ₂ O ₃ /ZnO	acetylene	120°C	200 ppm	96.46% ^②	-	-	1 ppm	9
ZnO/rGO	NO ₂	RT	50 ppm	9.61 ^①	25	15	5 ppm	10
CuO/rGO	NO ₂	RT	5 ppm	400.8% ^②	6.8	55.1	50 ppb	11
Pd-SnO ₂ /rGO	NO ₂	RT	100 ppm	7.92 ^①	56.9	22.1	37.8 ppb	12
CdS/CuO/rGO	NO ₂	RT	10 ppm	7.25 ^①	45.6	14.2	50 ppb	13
ZnO/ZrO₂	NO₂	RT	100 ppm	40.35^①	1.5 s	42.2 s	50 ppb	This work

20 ① :S = R_a/R_g or S = R_g/R_a

21 ② :S = |R_a-R_g|/R_a×100% or S = |R_g-R_a|/R_a×100%

22

23



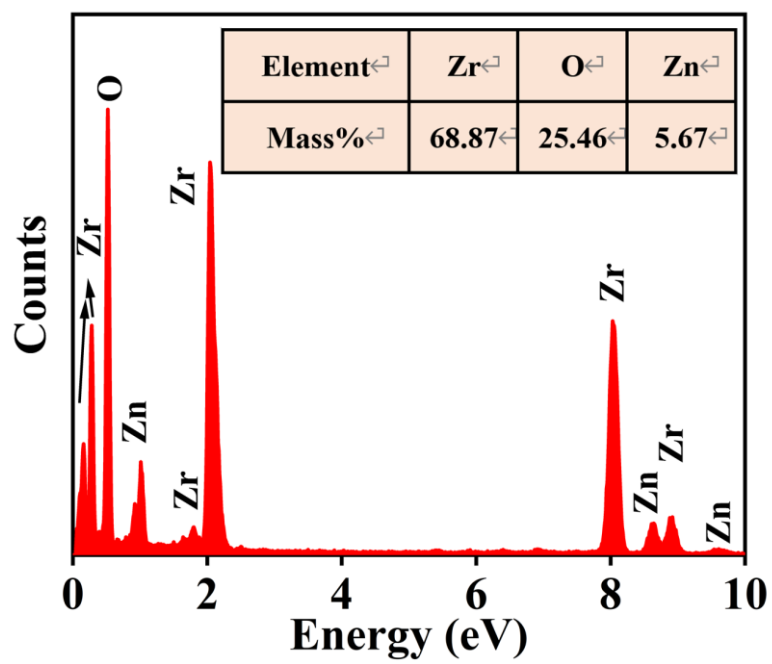
24

25

Fig. S1 (a) SEM images of UiO-66; (b) SEM images of ZrO₂.

26

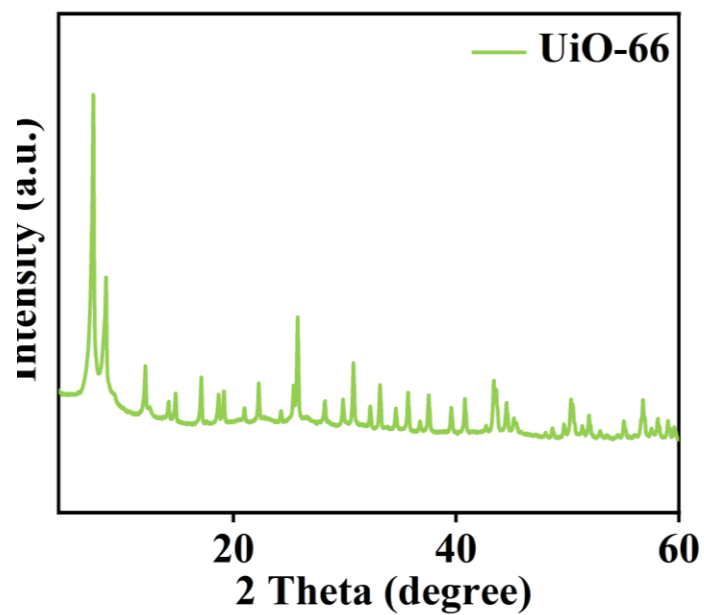
27



28

29

Fig. S2 EDS analysis of UZZ-2.



30

31

Fig. S3 PXR diagram of UiO-66.

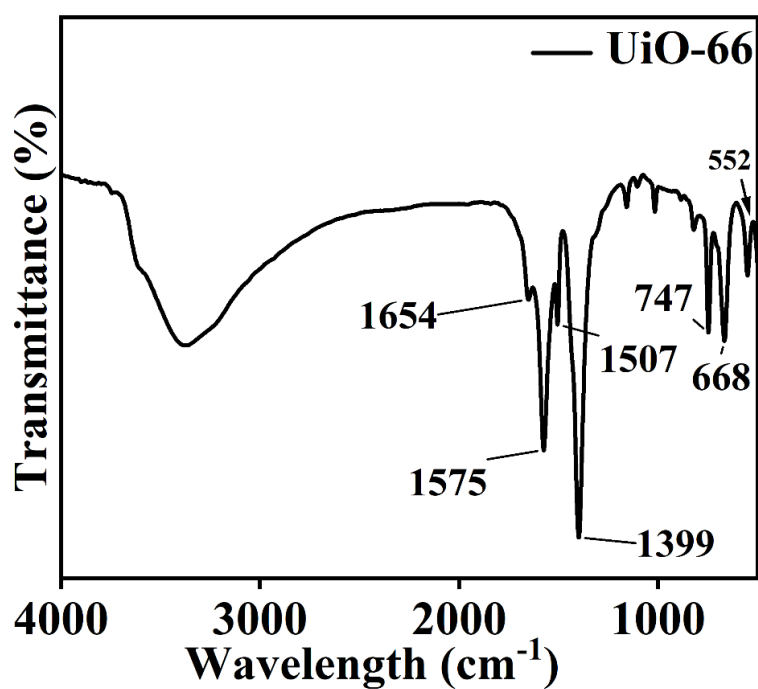
32

33

34

35

Fig. S3 shows the PXR diagram of the metal-organic skeleton UiO-66. Various characteristic peaks of UiO-66 observed at 7.5°, 8.6°, 26° and 31° index to the (111), (200), (600) and (731) planes, respectively, consistent with reported literature.^{14,15}



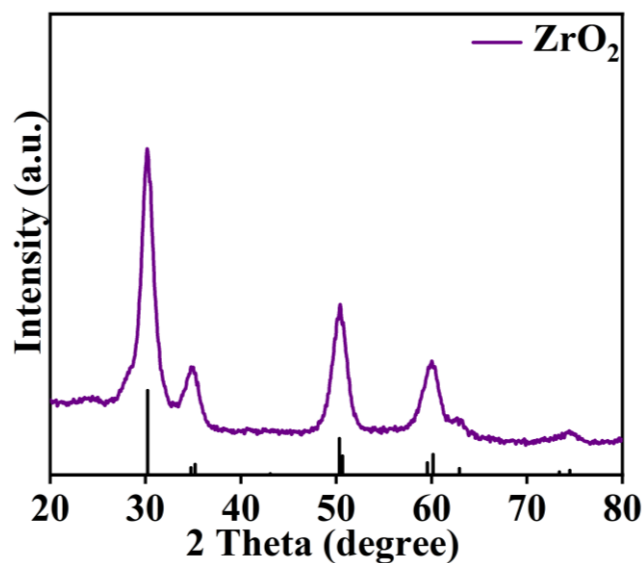
36

37

Fig. S4 FT-IR spectrum of UiO-66.

38 For the original UiO-66 sample, the strong characteristic peak at 3400 cm^{-1} comes
39 from the hydroxyl vibrations of the adsorbed H_2O molecules. The peak at 1654 cm^{-1} is
40 attributed to the bending vibration of $-\text{OH}$, and the two characteristic peaks at 1575 and
41 1399 cm^{-1} are the symmetric stretching vibration and the asymmetric stretching
42 vibration of the organic ligand $\text{O}-\text{C}=\text{O}$. The characteristic peak at 1507 cm^{-1} is the
43 vibrational peak of $\text{C}=\text{C}$ in the benzene ring, and at about 747 and 668 cm^{-1} are the
44 vibrational peaks typical of $\text{C}-\text{H}$ aromatic organic compounds. In addition, the
45 asymmetric stretching vibration peak of $\text{Zr}-(\text{OC})$ is at about 552 cm^{-1} .^{16,17}

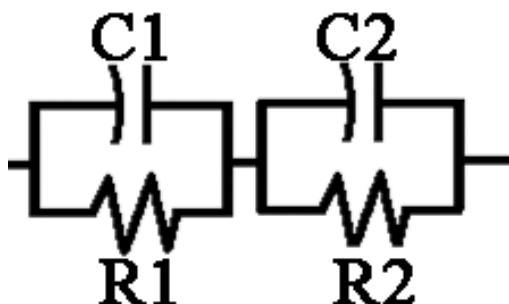
46



47

48

Fig. S5 XRD diagram of ZrO_2 .



49

50

Fig. S6 Equivalent circuit model for interpreting EIS data.

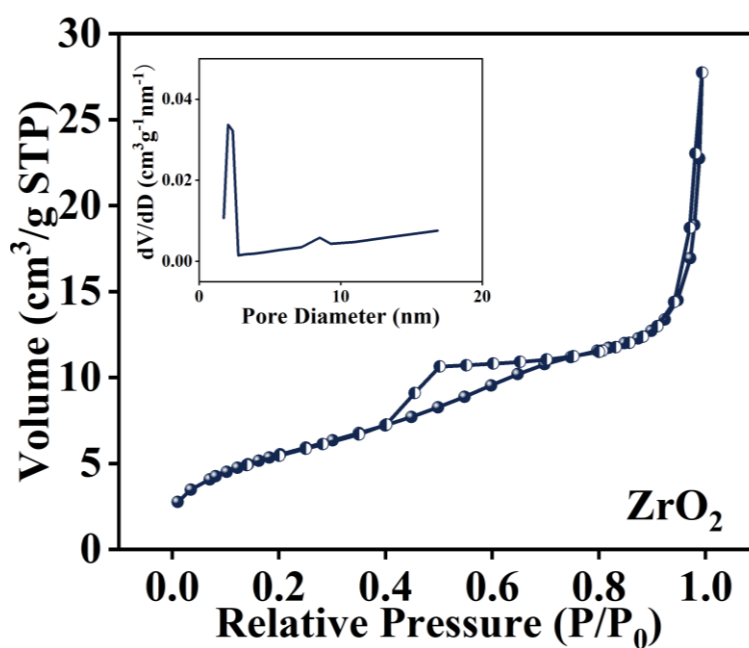
51 **Table S2** Parameters obtained by fitting the experimental curve to the equivalent circuit.

Raw materials	R ₁ (Ω)	C ₁ (F)	R ₂ (Ω)	C ₂ (F)
UZZ-2	8.367×10 ⁴	9.521×10 ⁻¹¹	1.874×10 ⁶	1.792×10 ⁻¹⁰
UZZ-1	2.062×10 ⁵	6.693×10 ⁻¹¹	1.101×10 ⁷	2.341×10 ⁻¹⁰
UZZ-3	2.436×10 ⁵	6.447×10 ⁻¹¹	9.455×10 ⁶	3.131×10 ⁻¹⁰
ZrO ₂	2.436×10 ⁵	6.447×10 ⁻¹¹	9.454×10 ⁶	3.131×10 ⁻⁹

52 Where R₁ is the resistance at the electrode/sample interface, C₁ is the associated
 53 capacitance. R₂ is mainly derived from the conductivity of the sample itself, and C₂ is
 54 the corresponding associated capacitive property of the material itself.

55

56



57

58 **Fig. S7** N₂ adsorption-desorption isotherms for pure samples of ZrO₂ (inset shows the pore size distribution curve).

59

60

61

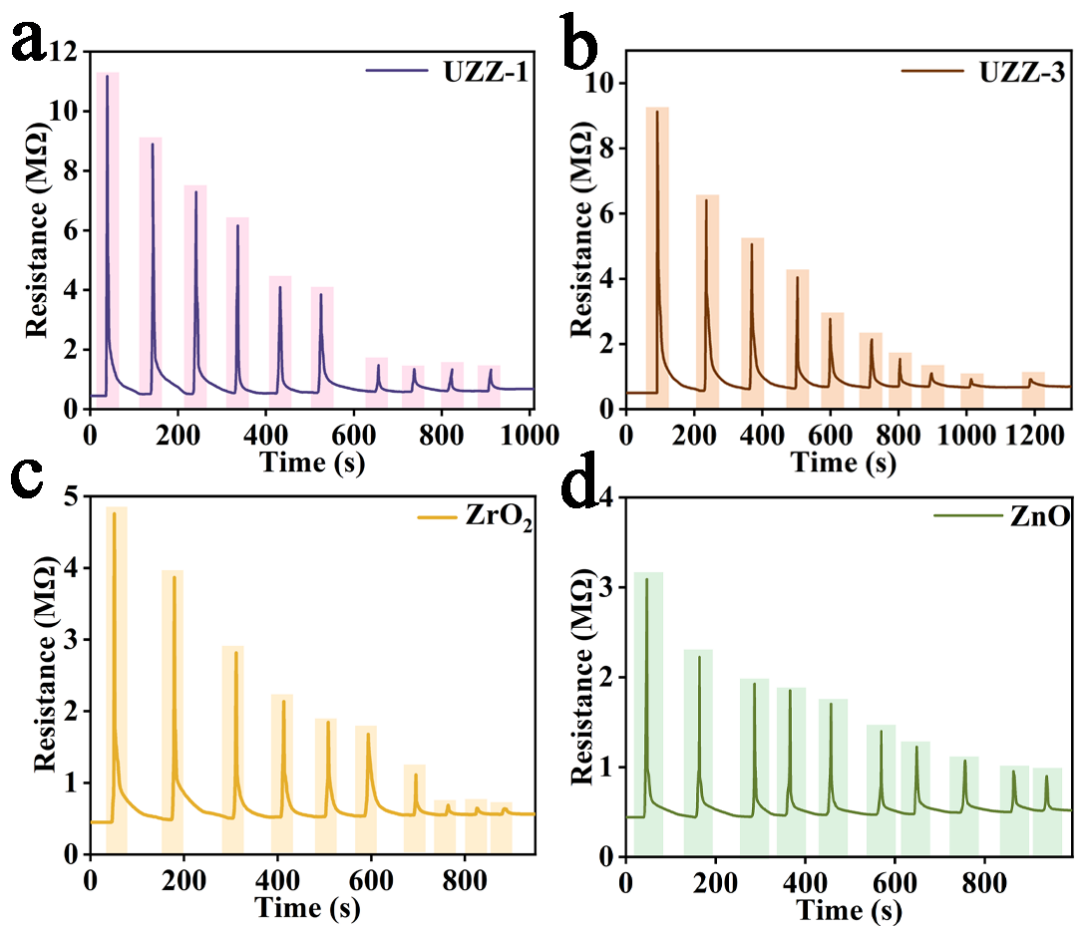
62 **Table S3** Sample BET surface area, average pore size and pore volume.

Sample	S_{set} ($\text{m}^2 \text{g}^{-1}$)	Pore Size (nm)	Pore Volume ($\text{cm}^3 \text{g}^{-1}$)
ZrO ₂	20.4676	9.5330	0.0429
UZZ-1	42.0633	4.4520	0.0606
UZZ-2	43.3205	5.8679	0.0801
UZZ-3	28.4719	6.2261	0.0511

63

64

65



66

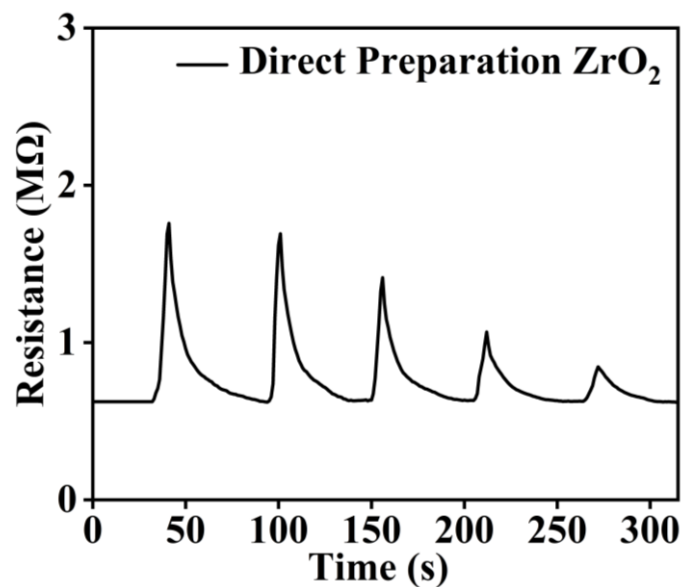
67 **Fig. S8** Response curves of (a) UZZ-1; (b) UZZ-3; (c) ZrO₂; (d) ZnO sensors at room temperature for different

68 concentrations of NO₂.

69 **Table S4** Response, response time and recovery time of samples at different NO₂ concentrations at room temperature.

Sample	UZZ-2			UZZ-1			UZZ-3			ZrO ₂			ZnO		
	NO ₂ (ppm)	S	Tres/s	Trec/s	S	Tres/s	Trec/s	S	Tres/s	Trec/s	S	Tres/s	Trec/s	S	Tres/s
100	40.35	1.40	42.20	24.84	4.80	77.50	18.25	6.40	89.40	10.57	7.20	98.00	6.99	5.30	59.20
50	37.39	2.30	38.50	17.31	5.50	70.80	11.07	6.80	60.60	7.96	8.10	95.10	5.02	6.20	56.80
30	34.39	3.20	36.30	14.16	6.90	67.20	8.21	7.50	54.20	5.62	9.20	48.30	4.17	7.40	38.00
10	27.97	4.70	32.80	11.31	7.60	51.30	6.34	7.80	43.50	4.04	10.20	32.40	3.99	8.50	36.40
5	22.14	6.10	29.60	7.20	8.20	39.80	3.86	9.50	28.80	3.49	15.20	30.20	3.43	9.20	28.50
3	17.63	7.30	28.30	6.79	10.40	36.40	3.05	10.60	23.50	3.12	16.10	21.30	2.92	10.20	25.00
1	13.14	10.80	22.40	2.49	11.60	15.00	2.20	13.20	21.20	2.01	23.30	15.40	2.53	10.80	23.60
0.5	9.19	11.90	20.00	2.24	13.40	11.40	1.56	15.40	19.30	1.24	24.80	5.80	2.12	11.20	21.40
0.3	7.01	12.80	17.00	2.11	15.20	7.60	1.35	17.50	6.20	1.14	25.50	3.60	1.90	15.40	18.10
0.1	4.59	13.00	13.80	1.47	17.30	3.30	1.13	19.20	4.30	1.09	25.80	3.20	1.73	16.20	13.40
0.05	2.69	14.70	8.50												

70 *S:Response T_{res}: Response time T_{rec}: Recovery time



71

72 **Fig. S9** The response curves of directly prepared ZrO₂ sensors towards different concentrations of NO₂ at room
73 temperature.

74

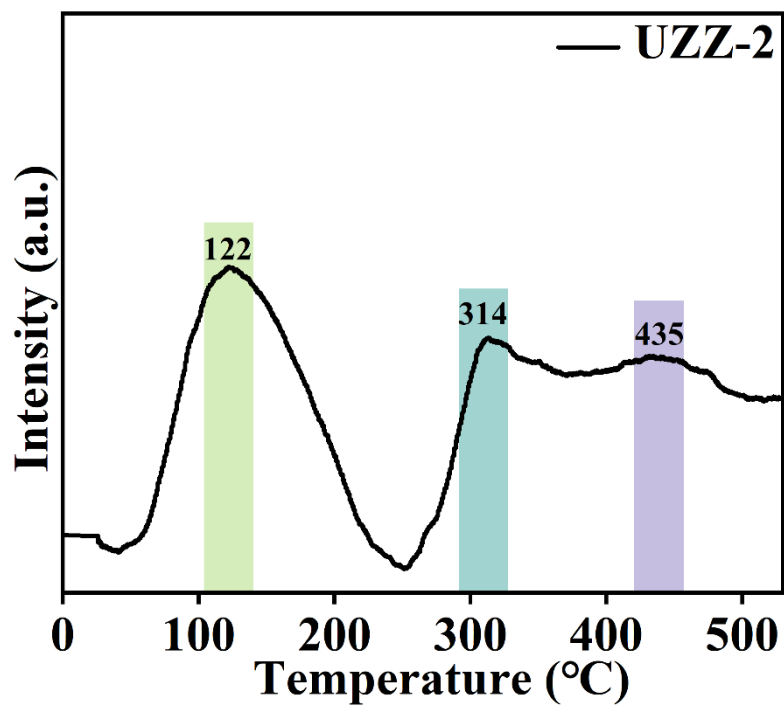
75

76 **Table S5** Peak position and peak area ratio of XPS O1s for UZZ-2 and UZZ-2+NO₂
77 samples (%).

Sample	UZZ-2			UZZ-2+NO ₂		
	O _i	O _v	O _c	O _i	O _v	O _c
Peak	O _i	O _v	O _c	O _i	O _v	O _c
Binding energy (eV)	530.7	531.5	532.7	530.8	531.7	532.8
Peak area ratio (%)	41.2	33.2	25.6	22.7	30.1	47.2

78

79



80

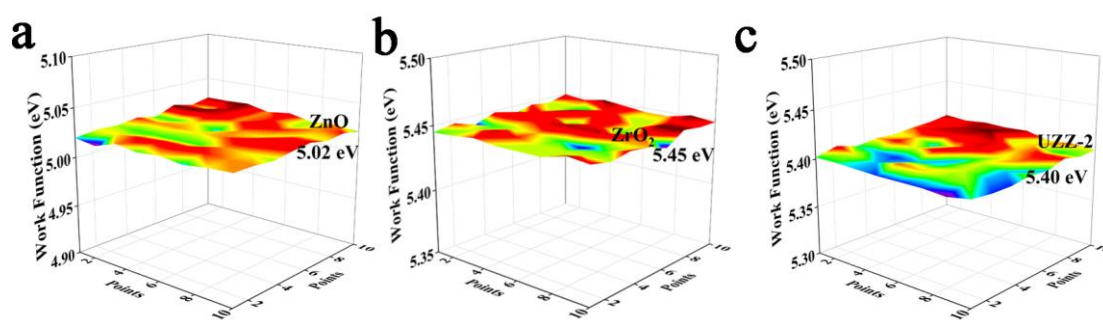
81

Fig. S10 NO₂-TPD of UZZ-2.

82

83

84

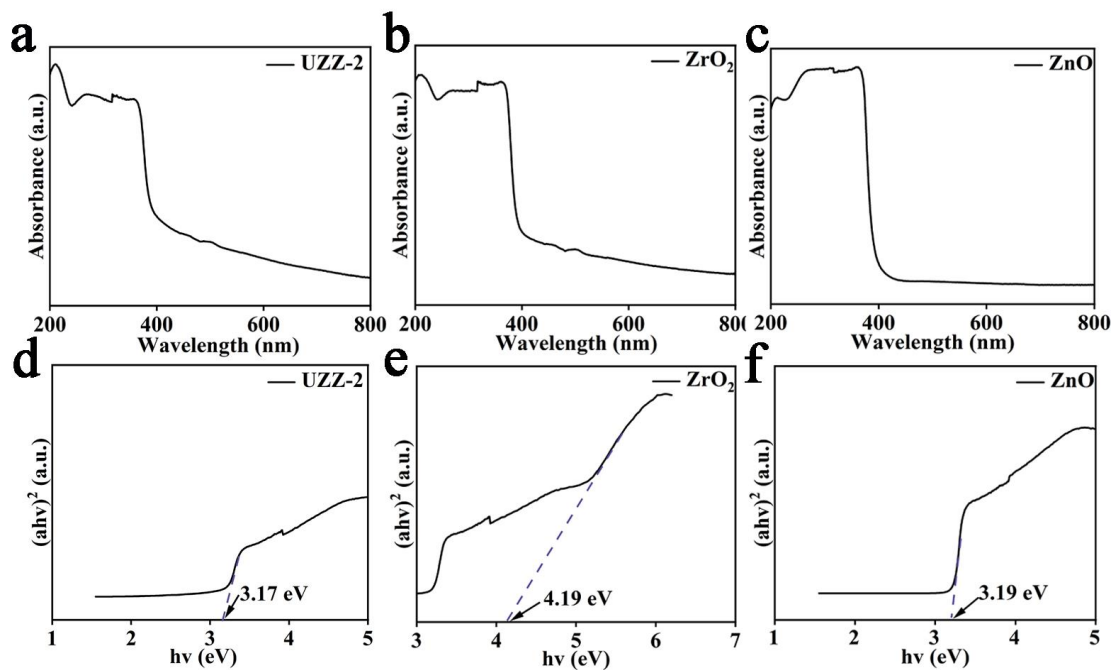


85

86

Fig. S11 Kelvin probe test of (a) ZnO; (b) ZrO₂; (c) UZZ-2.

87



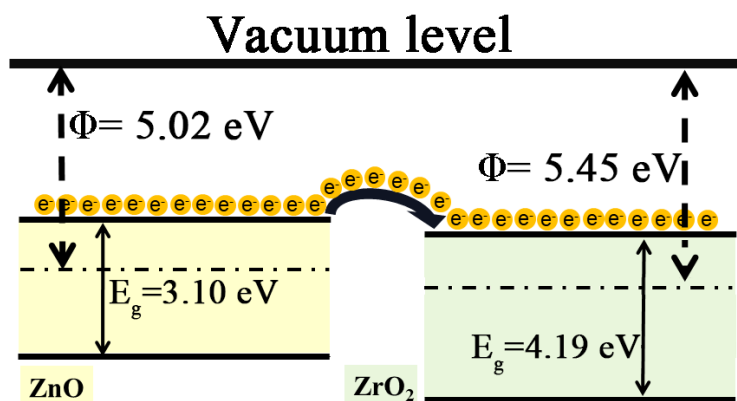
88

89 **Fig. S12** (a-c) UV-vis absorption spectra of UZZ-2, ZrO₂ and ZnO; (d-f) Tauc plots of UZZ-2, ZrO₂ and ZnO. (The

90 energy value at the intersection of the tangent line and the horizontal axis is the band gap width).

91

92



93

94 **Fig. S13** Schematic diagram of the work function of ZnO and ZrO₂.

95

96

97

98

99 **References**

- 100 1. J. H. Bang, N. Lee, A. Mirzaei, M. S. Choi, H. Choi, H. Jeon, S. S. Kim and H. W. Kim, *Sens.*
101 *Actuator B-Chem.*, 2020, **319**.
- 102 2. A. Ferlazzo, C. Espro, D. Iannazzo, K. Moulaei and G. Neri, *International Journal of*
103 *Hydrogen Energy*, 2022, **47**, 9819-9828.
- 104 3. G. Q. Feng, Y. H. Che, S. H. Wang, S. Q. Wang, J. Hu, J. K. Xiao, C. W. Song and L. L. Jiang,
105 *Sens. Actuator B-Chem.*, 2022, **367**.
- 106 4. C. M. Lou, Z. S. Li, C. Yang, X. H. Liu, W. Zheng and J. Zhang, *Sens. Actuator B-Chem.*,
107 2021, **333**.
- 108 5. L. Zhu, W. Zeng, J. D. Yang and Y. Q. Li, *Materials Letters*, 2018, **230**, 297-299.
- 109 6. R. S. Ganesh, M. Navaneethan, V. L. Patil, S. Ponnusamy, C. Muthamizhchelvan, S. Kawasaki,
110 P. S. Patil and Y. Hayakawa, *Sens. Actuator B-Chem.*, 2018, **255**, 672-683.
- 111 7. Y. Seekaew, S. Kamlue and C. Wongchoosuk, *Acs Applied Nano Materials*, 2023, **6**, 9008-
112 9020.
- 113 8. S. H. Kwon, T. H. Kim, S. M. Kim, S. Oh and K. K. Kim, *Nanoscale*, 2021, **13**, 12177-12184.
- 114 9. V. V. Kondalkar, L. T. Duy, H. Seo and K. Lee, *ACS Appl. Mater. Interfaces*, 2019, **11**, 25891-
115 25900.
- 116 10. Z. Liu, L. Yu, F. Guo, S. Liu, L. Qi, M. Shan and X. Fan, *Applied Surface Science*, 2017, **423**,
117 721-727.
- 118 11. H. Bai, H. Guo, J. Wang, Y. Dong, B. Liu, Z. Xie, F. Guo, D. Chen, R. Zhang and Y. Zheng,
119 *Sensors and Actuators B: Chemical*, 2021, **337**.
- 120 12. H. Bai, H. Guo, C. Feng, J. Wang, B. Liu, Z. Xie, F. Guo, D. Chen, R. Zhang and Y. Zheng,
121 *Applied Surface Science*, 2022, **575**.
- 122 13. F. Guo, C. Feng, Z. Zhang, H. Wu, C. Zhang, X. Feng, S. Lin, C. Xu, B. Zhang and H. Bai,
123 *Sensors and Actuators B: Chemical*, 2022, **364**.
- 124 14. D. W. Hu, X. J. Song, S. J. Wu, X. T. Yang, H. Zhang, X. Y. Chang and M. J. Jia, *Chinese*
125 *Journal of Catalysis*, 2021, **42**, 356-366.
- 126 15. X. X. Peng, L. Ye, Y. C. Ding, L. C. Yi, C. Zhang and Z. H. Wen, *Applied Catalysis B-*
127 *Environmental*, 2020, **260**.
- 128 16. C. Q. Chen, D. Z. Chen, S. S. Xie, H. Y. Quan, X. B. Luo and L. Guo, *ACS Appl. Mater.*
129 *Interfaces*, 2017, **9**, 41043-41054.
- 130 17. W. Xu, Z. H. Xu, W. X. Yao, L. H. Hu, K. Q. Ding, G. D. Wu, G. M. Xiao and L. J. Gao, *Applied*
131 *Catalysis a-General*, 2023, **662**.
- 132